

### 3-D Finite-Element Numerical Simulation of Centrifugal Induction Electroslag Casting Solidification Process

Xichun Chen, Deguang Zhou, Jie Fu, Weiguo Xu

Metallurgy School, University of Science and Technology Beijing, Beijing 100083, China  
(Received 2001-03-01)

**Abstract:** A 3-D finite-element numerical simulation model of temperature field for CIESC casting solidification process was developed with the aid of ANSYS software and a series of corresponding experiments were made. The results showed that the good agreement was obtained between the numerical simulation and the experiments. Based on the numerical simulation results, the characteristics of temperature distribution in the castings during CIESC solidification process were analyzed and summarized. According to the  $G/R^{1/2}$  method and numerical simulation results, there is no any shrinkage defect in the CIESC casting and structure of casting is fine and compact.

**Key words:** 3-D finite-element numerical simulation; ANSYS software; solidification process; centrifugal induction electroslag casting (CIESC); shrinkage defect

#### 1 Introduction

Centrifugal Induction Electroslag Casting (CIESC) is a new electroslag metallurgy technology to cast the shaped and hollow castings developed by the University of Science and Technology Beijing in the early of 1990's, which combined the virtues of electroslag induction melting and centrifugal casting [1]. Some products such as GCr15V cold extruding wheel, 4Cr5Mo-SiV1 ASSEL roller, 5CrMnMo hot compaction roller have been produced with the CIESC technology since 1994, and it has been proved by industrial applications that their service lives are 150%–300% as long as the same type of forging.

Till now, a lot of experiments have been carried out to study the mechanism of CIESC in order to develop more products and improve the mechanical and service properties of products further [2–5]. However, the liquid steel is wrapped in the molten slag and influenced by strong centrifugal force during solidification in CIESC case, and there is a large difference in cast structure compared with the solidification conditions of ESR and traditional centrifugal casting.

In this paper, the temperature field for CIESC solidification process is studied with numerical simulation based on the finite-element method using ANSYS / Mutiphases5.5.2 software in order to analyze its characteristics and optimize the technological parameters.

#### 2 3-D Finite-Element Numerical Simulation

A typical structure of CIESC system is shown as **fig-**

**ure 1.** There is a thin layer of slag skin between mould and casting, and its thickness is about 1–2 mm. It is a thin layer of slag that makes the liquid metal not contact directly with the mould wall and protects it. Due to the liquid steel is poured into the rotating mould together with molten slag, a thick layer of slag is gathered in the inner surface of casting. The section sizes of the CIESC system are shown in **table 1.**

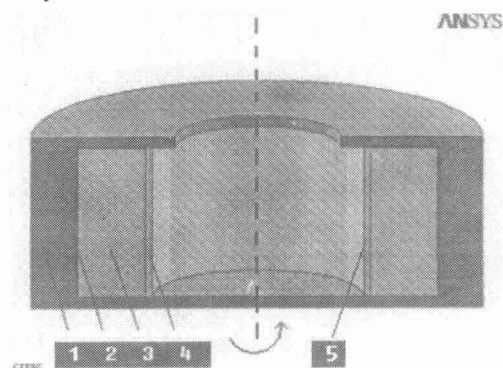


**Figure 1** Structure of CIESC casting, 1—mould; 2—slag skin; 3—casting; 4—inner slag layer; 5—free surface.

#### 2.1 Heat transfer equation and boundary conditions

Based on the energy conservation principle and Fourier heat transfer rule, the heat transfer differential equation of CIESC casting solidification process in pole coordinate system is:

$$\frac{\partial t}{\partial \tau} = \frac{\lambda}{\rho C_p} \left[ \frac{1}{r} \frac{\partial}{\partial r} \left( r \frac{\partial t}{\partial r} \right) + \frac{1}{r^2} \frac{\partial^2 t}{\partial \phi^2} + \frac{\partial^2 t}{\partial z^2} \right] + \bar{Q} \quad (1)$$

Where  $t$  is the temperature, °C;  $\tau$  the time, s;  $\lambda$  the coefficient of heat conductivity, W/(m°C);  $\rho$  the density,

Table 1 Section sizes of the CIESC system

mm

System	Outer diameter	Inner diameter	Height	Others
Mould	600	480	600	Thicknesses of upper cover plate and lower shoe are 30 mm; the diameter of sprue gate in upper cover plate is 220 mm.
Casting	479	300	448	
Slag skin thickness		1		
Inner slag layer thickness		10		

$\text{kg/m}^3$ ;  $C_p$  the specific heat capacity at constant pressure,  $\text{kJ/kg} \cdot ^\circ\text{C}$ ;  $\bar{Q}$  the solidifying latent heat,  $\text{W/m}^3$ .

The heat transfer during CIESC casting solidification process includes convection between outer wall of mould and atmosphere, convection between upper cover plate, lower shoe and atmosphere, natural convection and radiation heat transfer from the free surface of slag layer in casting free surface to atmosphere through sprue gate in the upper cover plate.

(1) Convection heat transfer between outer wall of mould and atmosphere.

Because of the quick revolution of mould, the convection between outer wall of mould and atmosphere is a kind of forced convection. According to the literature [6], the average coefficient of heat transfer can be obtained from the following equation:

$$Nu_m = CRe_m^n \quad (2)$$

where  $Nu_m$  is the Nusselt number at the qualitative temperature;  $Re_m$  the Reynolds number at the temperature;  $C, n$  the constants depended on the  $Re_m$ . When the revolution of mould is 900 r/min, the average coefficient of heat-transfer can be calculated under the conditions of the model,  $\alpha = 41.94 \text{ W}/(\text{m}^2 \cdot ^\circ\text{C})$ .

(2) Convection between upper cover plate, lower shoe and atmosphere.

Similarly, the convection heat transfer between upper cover plate, lower shoe and atmosphere may be treated as gas passing through a flat plate in the state of laminar flow. The average coefficient of heat transfer can be obtained from the following equation:

$$Nu = \frac{\alpha L}{\lambda} = 0.664 Re_L^{1/2} Pr^{1/3} \quad (3)$$

where  $Pr$  is the Prandtl number. When the revolution of mould is 900 r/min, the average coefficient of heat transfer can be calculated under the conditions of the model,  $\alpha = 26.43 \text{ W}/(\text{m}^2 \cdot ^\circ\text{C})$ .

(3) Natural convection through sprue gate.

The average natural convection coefficient of heat transfer from free surface of inner slag layer to atmosphere through sprue gate in the upper cover plate can be calculated according to the following equation:

$$Nu_m = C(Gr \cdot Pr)_m^n \quad (4)$$

Where  $Gr$  is the Grashof number. Under the condition of the model, the average coefficient of heat transfer is  $\alpha = 0.074 \text{ W}/(\text{m}^2 \cdot ^\circ\text{C})$ .

(4) Radiation through sprue gate.

The radiation heat transfer from free surface of inner slag layer to atmosphere through sprue gate in the upper cover plate can be calculated according to the Stefan-Boltzman equation:

$$Q = \varepsilon \sigma A_1 F_{12} (T_1^4 - T_2^4) \quad (5)$$

where  $\varepsilon$  is the emission ratio;  $\sigma$  the Boltzman constant;  $A_1$  the surface area of radiation;  $F_{12}$  is the number which can be determined from the following equation,

$$F_{12} = \frac{1}{F_1} \int_{F_1} \int_{F_2} \frac{\cos\theta_1 \cos\theta_2}{\pi r^2} dF_1 dF_2 \quad (6)$$

On the conditions of the model,

$$F_{12} = \frac{r_2^2}{r_1 H} - \frac{r_1 r_2^2}{H r_1^2 + H^3} \quad (7)$$

Where  $H, r_1$  and  $r_2$  are the height of inner slag layer, the radius of the free surface and the sprue gate respectively.

Materials involved in numerical simulation are L3 (casting), slag ( $\text{CaO-Al}_2\text{O}_3\text{-SiO}_2\text{-CaF}_2$ ) and A3 (mould). All thermal parameters of these materials refer to literature [7].

## 2.2 Solidifying latent heat

For the numerical simulation model, the method provided by ANSYS/Multiphysics was used to deal with the solidifying latent heat, which is to define the enthalpy as a function of temperature to account for the heat energy that system releases during solidification process. Enthalpy is calculated by equation (8).

$$H = \int p c(T) dT \quad (8)$$

## 2.3 3-D finite-element numerical simulation

Based on the symmetry, a half of the casting system is taken and meshed with the aid of ANSYS/Multiphysics, which is shown as **figure 2**. Then, all relevant thermal parameters, boundary conditions and initial conditions were inputted into the ANSYS/Multiphysics software as the software hinted.

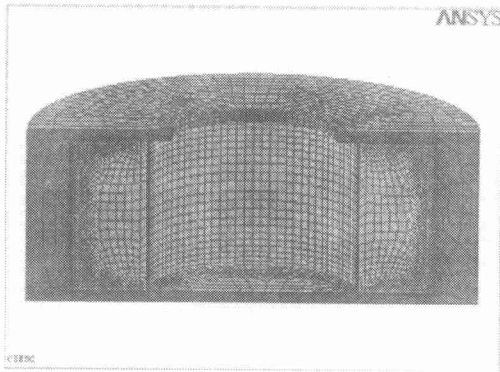


Figure 2 Model of CIESC system in calculation.

### 3 Confirmatory Test

In order to verify the results of numerical simulation, a series of corresponding experiments were made. The sketch of confirmatory test equipment was shown as figure 3. The temperature of mold in certain position was measured and recorded for every five second as soon as the liquid steel was poured into the mould together with the molten slag.

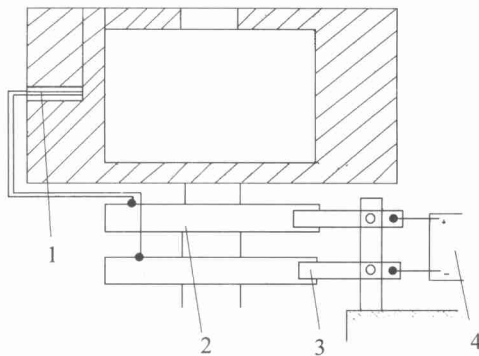


Figure 3 Sketch of confirmatory test equipment, 1—thermocouple; 2—brass ring; 3—brass brush; 4—potentiometer.

## 4 Result and Discussion

### 4.1 Result comparison of numerical simulation with confirmatory test

The temperature varying with time at the certain position in the mould during solidification process was drawn as figure 4. The curves 2 and 1 are drawn according to the results of experiments and corresponding numerical simulation respectively. For experiment No.1, the initial temperature of mould, liquid steel and molten slag are 130°C, 1560°C and 1650°C respectively, and for experiment No.2 that are 180°C, 1580°C and 1650°C respectively. From the comparison (figure 4), it is known that the good agreement was obtained between the numerical simulation and the experimental results.

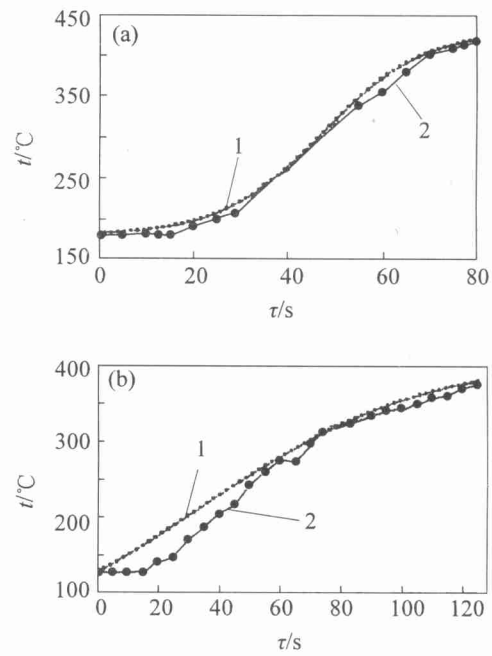


Figure 4 Comparison of the numerical simulation with experimental result, (a) experiment No.1; (b) experiment No.2; 1—calculated; 2—experimental.

### 4.2 Characteristics of temperature field during CI-ESC solidification process

Based on the numerical simulation results, the characteristics of temperature field distribution during CI-ESC solidification process are summarized as followings.

#### (1) Rapid solidification.

According to the experiment and numerical simulation results, in the CIESC L3 cylinder casting of outer diameter 478 mm, inner diameter 300 mm and height 418 mm, time solidified is within 167 min. The average solidifying and cooling rate are 3.47 mm/min and 0.176 °C/s. In the outside part of casting, the cooling rate is faster than the inside part. Figure 5 shows the temperature varying with time of the node in the center height

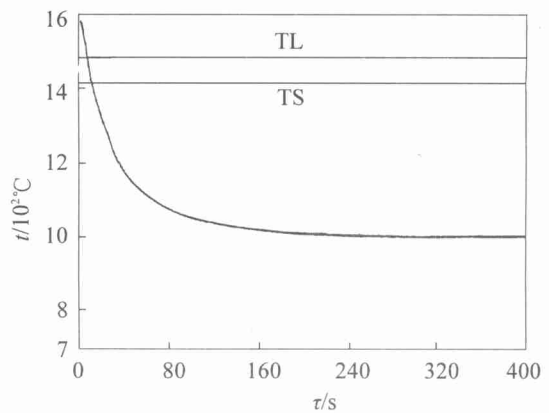
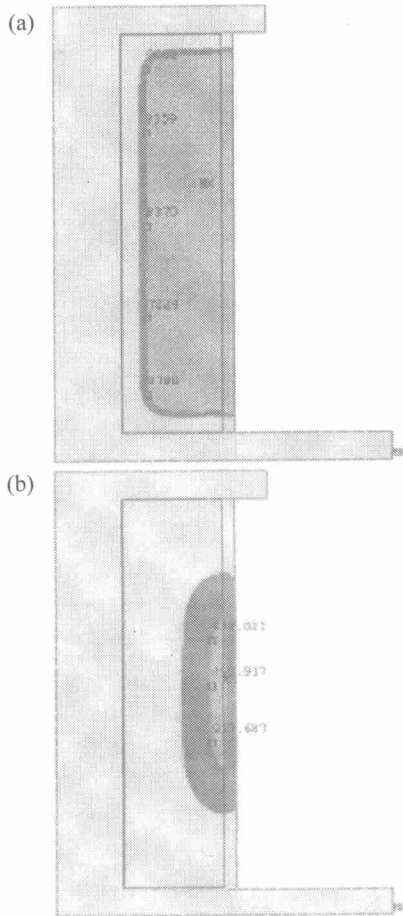


Figure 5 Temperature-time curve of a certain node in the outer part of casting.

and 12 mm away from outside surface of casting, from which it is shown that the average cooling rate in the liquid-solid two phase region is 6.1 °C/s, much higher than that of common sand casting and die cast, and even high to the level of water cooling solidification condition.

(2) Large solidifying condition difference.

During solidification process, there is large difference of solidifying condition between the outside part and inside part of CIESC casting. From **figure 6**, it is know that the temperature gradient of solidifying front



**Figure 6** Temperature gradient of solidifying front at 60 s (a) and 600 s (b).

in the outside part is about 8 000 °C/m, however, that is only 800 °C/m in the inside part. The large difference of solidifying condition will bring to unevenness of structure and performance between outside part and inside part of casting. **Figure 7** shows the macrostructure of CIESC L3 casting. The structure of inside part is coarser than that of outside part.

(3) Directional solidification.

During solidification process, the CIESC casting solidified directionally when there is enough molten slag gathering at the inside surface of casting, which is one of the virtues different from common centrifugal

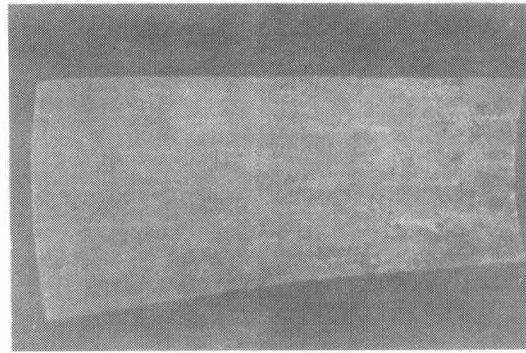


**Figure 7** Macrostructure of CIESC L3 casting.

casting. By the numerical simulation calculation, it is shown that 8mm molten slag can make the casting solidify directionally and the final solidified node will be in the molten slag under the calculation condition.

**4.3 Shrinkage Defect**

The main purposes of solidification numerical simulation is to know whether there will be shrinkage defect of casting and where the shrinkage defect is as well as how to avoid it. It is a complex procedure to forming shrinkage defect during solidification. Theoretically, it involves heat transfer in the liquid-solid two phase region, flow of liquid steel, pouring rate of liquid steel, and behavior of gaseous phase, and so on.

There are many methods to estimate the forming of shrinkage. According to the most current  $G/R^{1/2}$  method, there is existing shrinkage defect in the area where  $G/R^{1/2} < 1 (\text{°C} \cdot \text{min})^{1/2} \cdot \text{cm}^{-1}$ . **Figure 8** shows that the values of  $G/R^{1/2}$  are all more than  $1 (\text{°C} \cdot \text{min})^{1/2} \cdot \text{cm}^{-1}$ , which means there is no any shrinkage defect in the CIESC casting and its structure is fine and compacted. However, if there is not enough molten slag in the inner slag layer, two-direction solidification will take place and the final solidified area will be located within casting in the condition of 5 mm molten slag, showing in the **figure 9**. From the final solidified area, 82 mm

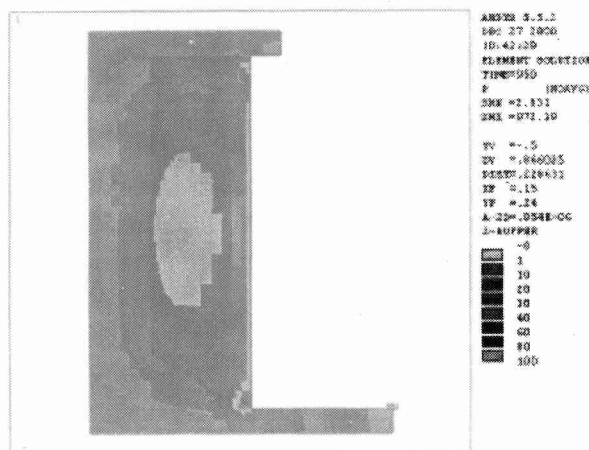


**Figure 8** Distribution of  $G/R^{1/2}$  value in the casting section.

away from outside surface and 7 mm away from inside surface, a piece of test sample was taken to examine by using an electronic scanner microscope. There are obvious microporosity and shrinkage defects in the sample, showing as **figure 10**. Therefore, a certain amount of molten slag is necessary to avoid shrinkage defect in CIESC process, which can be determined according to numerical simulation calculation and former experiences.

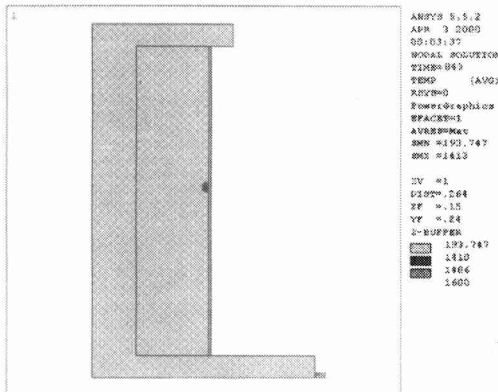


**Figure 9** Final solidified area when the thickness of inner slag layer is only 5 mm.

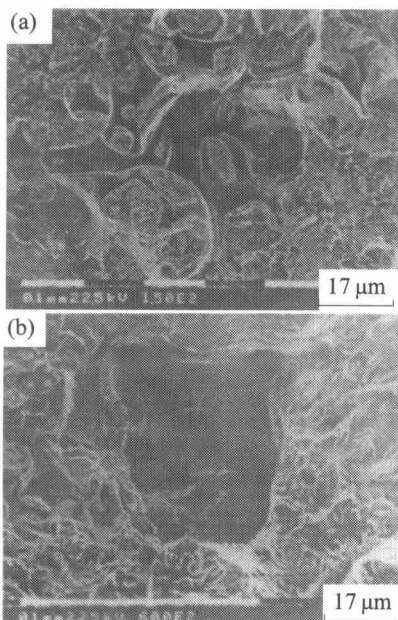


**Figure 10** Microporosity (a) and shrinkage defects (b) in the sample.

## 5 Conclusions

(1) A 3-D finite-element numerical simulation model of temperature field for CIESC casting solidification process was developed with the aid of ANSYS software and a series of corresponding experiments were carried out. The results showed that the good agreement was obtained between the numerical simulation and the experiments.

(2) Based on the numerical simulation results, the characteristics of temperature distribution field during CIESC solidification process are analyzed and summarized as: rapid solidification; large solidifying condition difference between the outside part and inside part of CIESC casting; directional solidification.

(3) According to the  $G/R^{1/2}$  method, there is no any shrinkage defect in the CIESC casting and its structure is fine and compacted. However, There are obvious microporosity and shrinkage defects in the casting if the thickness of the inner slag layer is not large enough, less than 10 mm calculated by the model under the experimental conditions.

## References

- [1] Z. Miao, W. Miao, J. Fu: [in] *Proceedings of the 1-th Pacific Rim International Conference on Advanced Materials and Processing*. France, 1992, p.47.
- [2] J. Fu, Z. Miao, W. Xu, et al: [in] *Proceedings of the 11-th ICVM*. France, 1992, p.174.
- [3] W. Xu, J. Fu, Y. Wang, et al: *Special Steel* (in Chinese), 16 (1995), No.5, p.42.
- [4] W. Xu, X. Chen, D. Zhou, et al: *J. Univ. & Tech. Beijing* (in Chinese), 20(1998), No.5, p.431.
- [5] J. Fu, W. Xu, Y. Wang, et al: *National Invention Patent* (China), No.91105455.3, 1998.
- [6] X. Zhang: *Metallurgy transfer principle* (in Chinese). The Metallurgical Industry Press, Beijing, 1987.
- [7] W. Xu: *Process and Theory Study of Centrifugal Induction Electroslag Casting*: [Doctor thesis]. Beijing: Univ. Sci. & Tech. Beijing, 1994, p.63.